

Experimental Validation of a Novel Compact Focusing Scheme for Future Energy-Frontier Linear Lepton Colliders

G. R. White,³ R. Ainsworth,¹⁵ T. Akagi,¹⁶ J. Alabau-Gonzalvo,² D. Angal-Kalinin,⁴ S. Araki,⁸ A. Aryshev,⁸ S. Bai,⁶ P. Bambade,¹⁴ D. R. Bett,⁵ G. Blair,^{15,18} C. Blanch,¹ O. Blanco,^{14,2} N. Blaskovic-Kraljevic,⁵ B. Bolzon,^{2,4,13} S. Boogert,¹⁵ P. N. Burrows,⁵ G. Christian,⁵ L. Corner,⁵ M. R. Davis,⁵ A. Faus-Golfe,¹ M. Fukuda,⁸ J. Gao,⁶ H. García-Morales,^{2,17} N. Geffroy,⁷ H. Hayano,⁸ A. Y. Heo,⁹ M. Hildreth,²⁰ Y. Honda,⁸ J. Y. Huang,¹⁰ W. H. Hwang,¹⁰ Y. Iwashita,¹¹ S. Jang,⁹ A. Jeremie,⁷ Y. Kamiya,¹² P. Karataev,¹⁵ E. S. Kim,⁹ H. S. Kim,⁹ S. H. Kim,¹⁰ Y. I. Kim,⁵ S. Komamiya,¹² K. Kubo,⁸ T. Kume,⁸ S. Kuroda,⁸ B. Lam,³ K. Lekomtsev,⁸ S. Liu,¹⁴ A. Lyapin,¹⁵ E. Marin,³ M. Masuzawa,⁸ D. McCormick,³ T. Naito,⁸ J. Nelson,³ L. J. Nevay,^{5,15} T. Okugi,⁸ T. Omori,⁸ M. Oroku,¹² H. Park,⁹ Y. J. Park,¹⁰ C. Perry,⁵ J. Pflugstner,² N. Phinney,³ A. Rawankar,⁸ Y. Renier,² J. Resta-López,¹ M. Ross,³ T. Sanuki,¹⁹ D. Schulte,² A. Seryi,⁵ M. Shevelev,⁸ H. Shimizu,⁸ J. Snuverink,¹⁵ C. Spencer,³ T. Suehara,¹² R. Sugahara,⁸ T. Takahashi,¹⁶ R. Tanaka,¹⁶ T. Tauchi,⁸ N. Terunuma,⁸ R. Tomás,² J. Urakawa,⁸ D. Wang,⁶ M. Warden,⁵ M. Wendt,² A. Wolski,¹³ M. Woodley,³ Y. Yamaguchi,¹² T. Yamanaka,¹² J. Yan,¹² K. Yokoya,⁸ F. Zimmermann²
(ATF2 Collaboration)

¹Universidad de Valencia - Instituto de Física Corpuscular (IFC), Edificio Institutos de Investigación, c/ Catedrático José Beltrán, 2, E-46980 Paterna, Spain

²European Organization for Nuclear Research (CERN), CH-1211 Geneva 23, Switzerland

³SLAC National Accelerator Laboratory, 2575 Sand Hill Road, Menlo Park, California 94025-7090, USA

⁴CLRC: Daresbury Laboratory, Daresbury, Warrington, Cheshire WA4 4AD, United Kingdom

⁵John Adams Institute for Accelerator Science at University of Oxford, Denys Wilkinson Building, Keble Road, Oxford OX1 3RH, United Kingdom

⁶Institute of High Energy Physics (IHEP), Chinese Academy of Sciences (CAS), Beijing, China

⁷LAPP-Universite de Savoie-CNRS/IN2P3, Annecy-le-Vieux, France.

⁸High Energy Accelerator Research Organization (KEK), 1-1 Oho, Tsukuba, Ibaraki 305-0801, Japan

⁹Department of Physics, Kyungpook National University, 1370 San Kyuk-dong, Puk ku, Taegu 635, South Korea

¹⁰Pohang Accelerator Laboratory, POSTECH (Pohang University of Science and Technology), San-31 Hyoja-dong, Pohang 790-784, South Korea

¹¹Institute for Chemical Research (ICR), Nuclear Science Research Facility, Kyoto University, Gokasho, Uji, Kyoto 611-0011, Japan

¹²Department of Physics, University of Tokyo, 7-3-1 Hongo, Bunkyo-ku, Tokyo 113, Japan

¹³Department of Physics, Oliver Lodge Laboratory, University of Liverpool, Oxford St., Liverpool L69 3BX, United Kingdom

¹⁴LAL, Universite Paris-Sud, CNRS/IN2P3, Orsay, France

¹⁵John Adams Institute for Accelerator Science at Royal Holloway University of London, Egham Hill, Egham, Surrey TW20 0EX, United Kingdom

¹⁶Department of Physics, Hiroshima University, 1-3-1 Kagamiyama, Higashi-Hiroshima 739-8526, Japan

¹⁷Universitat Politècnica de Catalunya, BarcelonaTech, C. Jordi Girona, 31. 08034 Barcelona, Spain

¹⁸Science and Technology Facilities Council, Polaris House, North Star Avenue, Swindon SN2 1SZ, United Kingdom

¹⁹Tohoku University, 28 Kawauchi, Aoba-ku, Sendai, 980-8576 Japan

²⁰University of Notre Dame, Notre Dame, Indiana 46556, USA

(Received 10 September 2013; published 24 January 2014)

A novel scheme for the focusing of high-energy leptons in future linear colliders was proposed in 2001 [P. Raimondi and A. Seryi, Phys. Rev. Lett. **86**, 3779 (2001)]. This scheme has many advantageous properties over previously studied focusing schemes, including being significantly shorter for a given energy and having a significantly better energy bandwidth. Experimental results from the ATF2 accelerator at KEK are presented that validate the operating principle of such a scheme by demonstrating the demagnification of a 1.3 GeV electron beam down to below 65 nm in height using an energy-scaled version of the compact focusing optics designed for the ILC collider.

DOI: 10.1103/PhysRevLett.112.034802

PACS numbers: 41.85.-p, 29.20.Ej, 29.27.-a

Designs for the next generation of energy-frontier lepton colliders envisage the generation and collision of particle beams into the TeV energy scale [1,2]. To deliver the required rate of particle interactions to the detectors for the

planned physics program, one of the most challenging technical aspects is the focusing and dynamic manipulation of the colliding particle bunches. A prototype final focus system (FFS) was constructed at the Accelerator Test

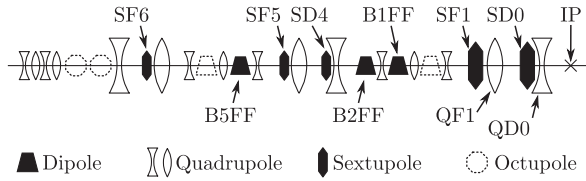


FIG. 1. Schematic of a final focus system with local chromaticity correction. Dashed components are not included in ATF2 test.

Facility (ATF) at KEK, Japan, with the primary goal of verifying a novel, so-called *local chromaticity correction* design first proposed in [3] (one of the earliest reviews of the chromatic compensation scheme can be found in [4]). The new design has many beneficial features over designs considered previously, the most notable being a considerable reduction in length. Both the proposed International Linear Collider (ILC) [1] and the Compact Linear Collider (CLIC) [2] consider this scheme in their baseline designs, although until now it has not been experimentally proven to be practically realizable. We report here results from the test accelerator ATF2 [5] taken during beam operations in 2012 and 2013. We have, on repeated occasions, reduced the 1.3 GeV electron vertical beam size down to approximately 70 nm and below, which has demonstrated the design feasibility.

A schematic of the optics layout is shown in Fig. 1. The complexity of the FFS is driven by the requirement to correct the dominant aberration necessarily present in any magnetic focusing optics: the chromaticity due to the strong final focusing magnets. The novelty of this design is to compensate for the chromaticity locally rather than using a separate optical section as considered previously. This is achieved by placing sextupoles (SD0 and SF1) adjacent to the final doublet quadrupoles which focus the beam and by intentionally introducing horizontal dispersion through

the FFS using dipole magnets. The parasitic second-order dispersion is canceled by arranging for an appropriate amount of residual chromaticity to leak from upstream sections. Higher order geometric and chromogeometric aberrations are corrected using additional upstream sextupoles and manipulating the optical transfer matrices between the magnetic elements according to the recipe outlined in [6]. Refinements to the initial design were performed using a global optimization procedure as proposed in [7]. This latest procedure uses a high-order transfer map using a *polymorphic tracking code* to fully compensate second and third order aberrations in the FFS in a semiautomated fashion.

The principal goal for ATF2 was to test the FFS design relevant to ILC. To achieve this, we designed a scaled version of the FFS optics that would present a level of difficulty to “tune” the beam at the focus point comparable to ILC. With magnet strength and focus length constrained by other design considerations, the difficulty to tune the beam is related to the level of demagnification demanded of the magnetic optics, which sets the chromaticity. The beam size at the focal point increases by an amount proportional to the product of the chromaticity and energy spread of the beam. This quantity is presented in Table I (fifth line) for ILC, CLIC, and ATF2, where one can observe that FFS designs with tighter focusing requirements (smaller focal point betatron functions) lead to optics which enlarge the beam size more due to chromatic growth and require tighter control of these and other resulting aberrations. A test facility used to demonstrate the previous focusing design (FFTB [8]) is also shown for comparison. The tuning difficulty manifests itself through the required precise balancing of high-order terms in the magnetic transport lattice. The precision required for the cancellation of these effects increases with the chromaticity, which places increasing demands on the placement tolerances of the magnets as well as their magnetic field settings and quality.

TABLE I. Key FFS parameters for ILC, CLIC, ATF2, and FFTB. L^* is the distance from QD0 to the focus point, ε_y the vertical emittance, ξ_y the vertical chromaticity, σ_E is the rms energy spread, σ_y the rms vertical beam size, and β^* the focal point beta function. The “pushed” optics demonstrates the tightest focusing possible by the ATF2 machine and is of future interest to show performance in conditions more applicable to the CLIC collider design [10].

	ILC (TDR 500 GeV)	ATF2	FFTB	ATF2 (pushed)	CLIC (CDR 3 TeV)
L^* (m)	3.5/4.5 ^a	1	0.4	1	3.5
ε_y (pm rad)	0.07	12	22	12	0.003
$\xi_y \sim (L^*/\beta_y^*)$	7,300/9,400 ^a	10,000	4,000	40,000	50,000
σ_E (%)	0.07/0.12 ^b	0.08	0.1	0.08	0.3
$\Delta\sigma_y/\sigma_y \sim (\sigma_E L^*/\beta_y^*)$	5/9, 7/11 ^{ba}	8	4	32	150
σ_y (nm) <i>design</i>	5.9	37	52	23	1
σ_y (nm) <i>measured</i>	-	65 ± 5 ^c	70 ± 6	-	-
β_x^* (mm)	11	4 (40°)	10	4	4
β_y^* (mm)	0.48	0.1	0.1	0.025	0.07

^aSiD/ILD ILC detector configurations.

^bPositron/electron side of ILC.

^cMarch 2013 results and configuration of ATF2 with bunch charge 80–130 pC.

When one calculates these tolerances (as for ATF2 in [9]), it is apparent that the tolerances are beyond our ability to achieve through standard survey and magnet engineering capabilities (with some magnets requiring submicron placement and/or few parts-per-million field strength settings). For the optics to work as required, we are reliant upon a series of complex online beam tuning procedures outlined below.

The ATF2 experimental FFS was constructed as a new extraction beam line to the existing ATF damping ring (DR) facility at KEK and was completed in December 2008. The ATF DR is a ~ 140 m circumference electron ring fed by an *s*-band linear accelerator which is used to accelerate the electron bunches produced by an rf gun to 1.3 GeV. In the normal ATF2 mode of operation, the DR delivers bunches of electrons with 1.6 nC charge at 3.12 Hz to the extraction system with typically measured (corrected) emittances of $2 \text{ nm rad} \times 12 \text{ pm rad}$ (horizontal and vertical dimensions, respectively). ATF2 is also used as a general-purpose R&D facility, with emphasis on the development of state-of-the-art beam diagnostic devices applicable for use in the next generation of linear colliders. Another noteworthy aspect of ATF2 is the unique way it is managed and operated in an international context: hardware construction, support and operation, operations shifts, software controls, and data analyses were all achieved through a collaborative international team spread across a globally diverse set of institutes.

The ATF2 beam line contains seven dipoles, three septa, 49 quadrupoles, five sextupoles, four skew sextupoles, and 25 corrector magnets. The quadrupoles and dipole bends for the main part of the FFS were purpose designed and built for ATF2, whilst the other magnets were reused from the old ATF extraction line and from the FFTB experiment at SLAC [11]. The beam line can be considered to consist of two sections: the extraction line (EXT) and the FFS. These are depicted in Fig. 2 which also shows the locations of key diagnostic and correction systems. The EXT is used for the extraction and manipulation of the beam out of the DR and preparing it for injection into the FFS beam line, i.e., for correcting residual energy dispersion, cross-plane coupling, and any mismatch from design in the phase space of the incoming beam.

The floor of ATF has been specially prepared, with deep concrete piles, to be vibrationally stable and have a good coherence length (~ 4 m for relevant frequencies). Additionally, work has been undertaken to ensure the

stability of the final doublet (FD: SF1, QF1, SD0, and QD0) support table [12]. The FD elements are attached to a rigid honeycomb block and bolted to the floor, using a thin layer of beeswax between the steel plate support at the base of the block and the floor to ensure good mechanical coupling. Measurements were made demonstrating the relative vibrations between QF1, QD0, and the focal point were within tolerance ($\sim < 10$ nm). A new design of high accuracy, high availability power supply system was installed [13] to satisfy the main field tolerances for ATF2 magnets [9] and to test the high availability requirements for future linear collider magnets. Each quadrupole and sextupole magnet in the FFS was mounted on a 3-axis mover system (horizontal, vertical, and roll directions) [14]. This system is used to align the FFS using the beam, to counter thermal drift, long-period ground motion, etc., and to calibrate the attached cavity beam position monitors (BPMs).

The beam orbit is monitored by a system of stripline (EXT, resolution $1\text{--}5 \mu\text{m}$ [15]), *c*- and *s*-band cavity (FFS, resolution $40\text{--}200 \text{ nm}$ [16]) BPMs. Also, there is a doublet of *c*-band cavities at the focal point with a demonstrated resolution of $< 5 \text{ nm}$ [17]. The key properties of the BPMs are high resolution, charge independence, and gain stability ($\sim 1\%$ per run period).

The tuning process starts within the EXT [18]: During the extraction process from the DR, the beam develops cross-plane coupling as well as horizontal and vertical energy dispersion that is outside the acceptance bandwidth of the FFS. The energy dispersion is corrected using a pair of quadrupole magnets and a pair of skew-quadrupole magnets within the dispersive part of the EXT. Changes in incoming beam phase space and cross-plane coupling are measured using a system of four beam profile devices which measure the optical transition radiation produced when the beam passes through thin metallic targets sequentially inserted into the path of the beam [19]. This system is capable of measuring and correcting the incoming vertical emittance at the 10% level. The phase space is corrected using an online beam model to adjust nine quadrupole magnets in the beginning section of the EXT. The coupling correction is especially important given the high horizontal to vertical aspect ratio of the beam (270:1 at the FFS focal point). To correct the coupling, the online model is used to compute a correction using four skew-quadrupole magnets in the EXT. The energy dispersion is typically corrected below 5 mm everywhere and

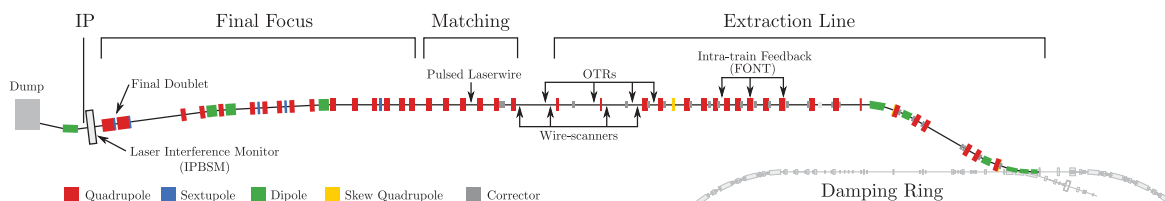


FIG. 2. The extraction line and final focus section of ATF2 after extraction from the damping ring.

the coupling corrected such that the measured beam ellipses on the optical transition radiation screens are corrected at the 0.1 degree level, and the beam phase space (matching) corrected to a *BMAG* [20] mismatch parameter of better than 1%. Simulations have shown this level of correction (the process and accuracy is similar to the simulated correction in the ILC beam delivery system) to be adequate for the FFS tuning to be successfully applied.

The tuning of the FFS ([18,21]) starts with the process of beam-based alignment. This utilizes the magnet movers, correction dipole magnets, and BPMs to align the beam close to the magnetic field centers of the magnets whilst ideally maintaining a straight beam trajectory through the whole system. It is especially important to have an orbit initially close to the field centers of the sextupole magnets. This is achieved by making use of the parabolic orbit response to horizontal and vertical motion of the sextupole magnets. Also of importance during the beam-based alignment procedure is achieving a beam orbit well centered in areas of the beam line with discontinuities to minimize wakefield effects. Careful steering was also important to minimize background signals in the focal point beam size monitor detectors. First-order correction for aberrations remaining directly at the focal point are performed by changing the field strength and rotation angles of the FD quadrupoles. This coarsely corrects for offset of the horizontal and vertical waist and energy dispersion at the focal point, and also for coupling. Following the tuning procedures described thus far typically yields a horizontal spot size of around 10 μm , close to the design value, and a vertical size of between 1 and 3 μm at the FFS focal point. At this stage, the focal point beam size measurements are performed using a carbon wirescanner (diameter $\sim 5 \mu\text{m}$).

Monte Carlo style simulations of the complete tuning process, including the final spot size tuning described below, have been performed by multiple people independently using different simulation programs to verify the tuning process. The simulations have demonstrated that the FFS should be tuneable following the procedures that are outlined here. Descriptions of the simulation process which also further describe the various tuning steps can be seen in [21,22]. Similar simulation efforts have been performed for the ILC and CLIC colliders [23]. It is through these simulations that confidence in the ability of this FFS design to generate the desired beam conditions in future collider facilities is reached. Therefore, the ongoing efforts to use the data from ATF2 to validate these simulations are considered important.

Before final tuning, the vertical beam size is dominated by the linear aberrations of waist shift (the focal point displaced longitudinally), energy dispersion, and coupling of the particle's horizontal angle at the focal point to vertical position. We also expect, and observe, second-order coupling and chromatic coupling terms to be present. Tuning knobs devised to remove the expected sources of linear beam

size aberrations are constructed using deliberate horizontal and vertical moves of the FFS sextupole magnets to construct orthonormal knobs. Four skew-sextupole magnets were added to control second-order terms and loosen the tolerances on higher-order field terms in the quadrupole magnets.

To perform the final tuning of the vertical spot size at the focal point from $\mathcal{O}(1 \mu\text{m})$ down to the design 37 nm, we use a unique beam size measurement device, referred to as a *Shintake Monitor* [24]. This is installed at the ATF2 focal point and is a highly improved version of the original, first used at FFTB [8]. It forms a vertically-orientated laser interference pattern at the electron beam focal point, which is scanned across the beam by altering the path length of one arm of the laser interferometer to scan the phase of the interference pattern. The beam size is inferred from the modulation of the resulting Compton scattered photon signal detected by a downstream CsI calorimeter-type photon detector. The *modulation depth* (M) of the signal is written as a function of the laser crossing angle and electron beam spot size:

$$M = C |\cos \theta| \exp[-2(k_y \sigma_y)^2],$$

$$k_y = \pi/d, d = \frac{\lambda}{2 \sin(\theta/2)},$$
(1)

where λ is the laser wavelength, θ is the laser crossing angle, and d represents the fringe pitch which determines the beam size range that can be measured. The correction factor C is included to express any contrast reduction of the laser fringe pattern due to mismatch of the laser overlap, distorted laser profile, etc. Multiple possible error sources inherent to the Shintake Monitor measurement process can also be included into this correction factor.

There are three possible collision modes for the Shintake Monitor (made available by adjusting the crossing angle between the interfering laser beams): 2° to 8° (continuously variable), 30° , and 174° . Mode switching is possible remotely and allows for continuously tuning the electron beam from a few micrometers down to a theoretical minimum of about 20 nm. An example modulation scan performed after beam tuning, in the 174° mode of operation, is shown in Fig. 3.

The results from three separate attempts to tune the beam in the ATF2 FFS beam line are summarized in Fig. 4. The entries in the histograms have unity C correction factors and represent an upper limit on the achieved vertical beam size [25]. As shown by these results, we demonstrate a capability for repeated tuning of the vertical beam size to around 70 nm and below using iterations of the tuning techniques described above. This should be compared with a calculated beam size of 450 nm without the use of sextupoles for local chromaticity correction. Rescaled to the nominal ILC beam energy of 250 GeV, these results correspond to a vertical beam size of about 5 nm (below the

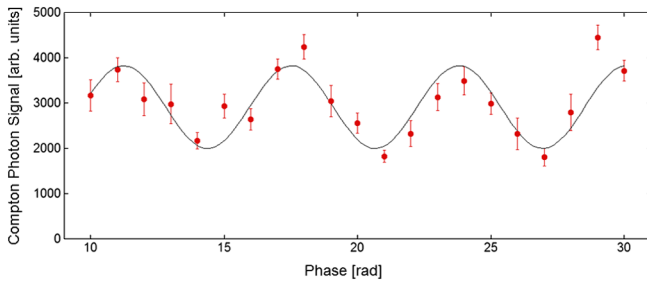


FIG. 3 (color online). Vertical beam size measurement (14th March 2013). Compton photon signals are measured as a function of the Shintake Monitor fringe phase with a crossing angle of 174° . The phase between the maxima of 2π corresponds to 266 nm. The beam size is 64.4 nm from the modulation depth ($M = 0.314$) without any systematic error correction applied.

baseline ILC design criteria). This confirms the practical operability of this optics design and the associated tuning procedure.

Studies are ongoing to identify the systematic effects contributing to the remaining ~ 30 nm of reduction required to reach the betatron limited beam size given by the optics design of 37 nm. We single out our two major contributing systematic effects here: wakefields and jitter effects in the Shintake Monitor. The beam is especially sensitive to wakefields (an order of magnitude more than expected at ILC) due to the long bunch lengths at ATF2 (6–10 mm)

and considerably lower beam energy. We express the wakefield contribution to the measured beam size as $\sigma_y^2 = \sigma_y(0)^2 + w^2 q^2$, where $\sigma_y(0)$ is the zero-charge (no wakefield effect) beam size, w the wakefield contribution, and q the bunch charge in nC. We have measured wakefield contributions of between 100–140 nm nC $^{-1}$ [18]. To minimize the effect on the beam size we operated at the lowest possible charges: between 80 and 200 pC. Work is ongoing to identify the wakefield sources and engineer solutions to mitigate them [26]. The beam size calculation is subject to systematic errors associated with the Shintake Monitor measurement and the complex interplay between these systematic effects and the beam tuning procedure. Error sources considered include those arising from phase jitter between the Shintake Monitor fringe pattern and the electron beam. This can be due to position jitter of the incident electron beam as well as spatial and temporal jitter sources within the laser system itself. Vertical jitter (statistical errors, background fluctuation, and laser timing errors, etc.) and horizontal jitter (where the signal is attenuated by varying power levels in the laser fringe) are present, with the latter responsible for degradation of the modulation depth. For a full treatment of Shintake Monitor error sources, see [25]. The relative phase jitter between the fringe pattern and the electron beam has been estimated by comparing measurements and simulations: this could account for about 10 nm in the beam sizes measured in 174° mode.

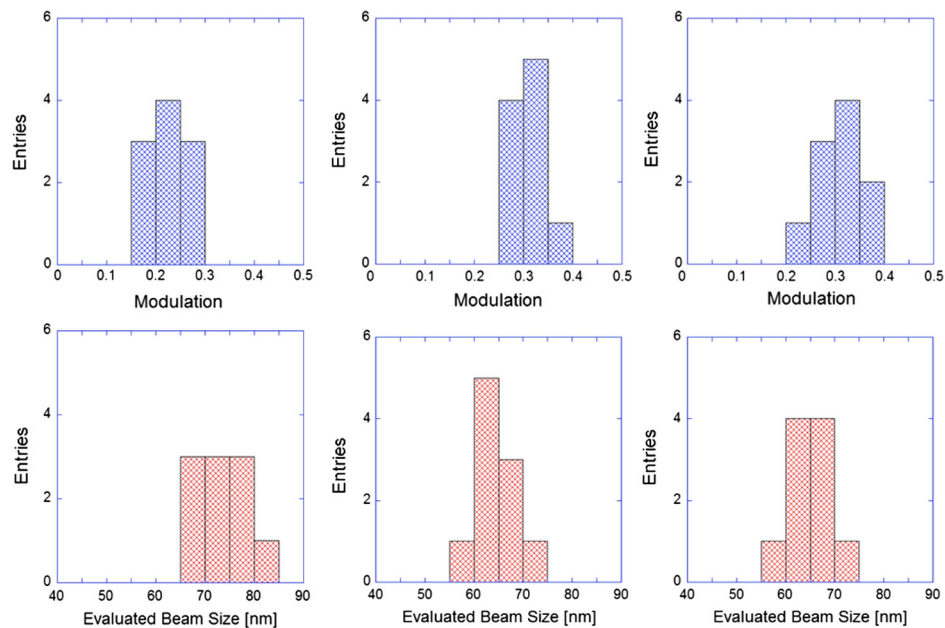


FIG. 4 (color online). Ten consecutive beam size measurements for each of the run periods: December 21, 2012 (left), March 8, 2013 (center), March 14, 2013 (right). The measured modulation depths shown on the top row are: 0.23 ± 0.05 , 0.31 ± 0.04 , and 0.30 ± 0.04 which correspond to beam sizes of: 73.2 ± 5.2 , 64.9 ± 3.5 , and 65.2 ± 4.0 nm, respectively (these represent upper limits: no systematic error correction applied). The measured beam charges for these data taking periods were < 200 , 100–130 and 80–100 pC, respectively.

The authors would like to acknowledge and thank the tireless work of the administration staff, engineers, and operations contract personnel of ATF2 who have made the construction and operation of the ATF2 facility possible. We also acknowledge and thank KEK management and support staff for their support of this international project. Work also supported in part by Department of Energy Contract No. DE-AC02-76SF00515 and US National Science Foundation Grant No. NSF-PHY 0935296 and Spanish Research Project No. FPA2010-21456-C02-01. We also acknowledge the support of the Agence Nationale de la Recherche of the French Ministry of Research (Programme Blanc, Project No. ATF2-IN2P3-KEK, Contract No. ANR-06-BLAN-0027).

-
- [1] T. Behnke *et al.*, [arXiv:1306.6327](https://arxiv.org/abs/1306.6327). See also <http://www.linearcollider.org/ILC/TDR> for a full list of contributing institutes.
- [2] M. Aicheler, P. Burrows, M. Draper, T. Garvey *et al.*, A Multi-TeV Linear Collider Based on CLIC Technology, 2012.
- [3] P. Raimondi and A. Seryi, *Phys. Rev. Lett.* **86**, 3779 (2001).
- [4] K. Brown and R. Servranckx, SLAC-PUB:3381, 1984.
- [5] B. I. Grishanov *et al.* (ATF2 Collaboration), ATF2 Proposal, 2005.
- [6] A. Seryi, M. Woodley, and P. Raimondi, SLAC-PUB-9895, 2003.
- [7] R. Tomás, *Phys. Rev. ST Accel. Beams* **9**, 081001 (2006).
- [8] V. Balakin, V. Alexandrov, A. Mikhailichenko, K. Flottmann, F. Peters *et al.*, *Phys. Rev. Lett.* **74**, 2479 (1995).
- [9] B. Grishanov, P. Logachev, F. Podgorny, V. Telnov, D. Angal-Kalinin *et al.*, ATF2 proposal. Vol. 2, 2006. Full proposal can be downloaded from http://atf.kek.jp/collab/md/projects/project_atf2.php.
- [10] E. Marin, R. Tomás, P. Bambade, K. Kubo, T. Okugi, T. Tauchi, N. Terunuma, J. Urakawa, A. Seryi, G. White, and M. Woodley, “Design and High Order Optimization of the Accelerator Test Facility 2 Lattices”, (to be published) in *Phys. Rev. ST Accel. Beams*.
- [11] C. M. Spencer, R. Sugahara, M. Masuzawa, B. Bolzon, and A. Jeremie, *IEEE Trans. Appl. Supercond.* **20**, 250 (2010).
- [12] B. Bolzon, in Conf. Proc. LCWS2007 C0705302, ATF201 (2007).
- [13] A. Bellomo, C. Lira, B. Lam, D. MacNair, and G. White, SLAC-PUB-13278, (2008).
- [14] G. Bowden, P. Holik, S. Wagner, G. Heimlinger, and R. Settles, *Nucl. Instrum. Methods Phys. Res., Sect. A* **368**, 579 (1996).
- [15] E. Medvedko, R. Johnson, S. Smith, and G. White, Conf. Proc. BIW2010-TUPSM027 (2010).
- [16] Y. Kim, R. Ainsworth, A. Aryshev, S. Boogert, G. Boorman *et al.*, *Phys. Rev. ST Accel. Beams* **15**, 042801 (2012).
- [17] Y. Kim, H. Park, S. Boogert, J. Frisch, D. McCormick *et al.*, Conf. Proc. IPAC-2011-TUPC119 C110904, 1296 (2011), to be published in the Journal of Instrumentation.
- [18] T. Okugi *et al.* (ATF2), Final focus system for linear colliders, ICFA Beam Dynamics Newsletter (2013).
- [19] J. Alabau-Gonzalvo, C. B. Gutierrez, A. Faus-Golfe, J. Garcia-Garrigos, J. Resta-Lopez *et al.*, Conf. Proc. IPAC-2012-MOPPR044 **C1205201**, 879 (2012).
- [20] M. Minty and F. Zimmermann, in *Measurement and Control of Charged Particle Beams* (Springer, New York, 2003), p. 113.
- [21] T. Okugi, S. Araki, P. Bambade, K. Kubo, S. Kuroda, M. Masuzawa, E. Marin, T. Naito, T. Tauchi, N. Terunuma, R. Tomás, J. Urakawa, G. White, and M. Woodley, “Linear and Second Order Optics Correction of Atf2 Final Focus Beamline” (to be published) in *Phys. Rev. ST Accel. Beams*.
- [22] G. R. White, S. Molloy, and M. Woodley, SLAC-PUB-13303, Conf. Proc. EPAC08-MOPP039, C0806233, MOPP039 (2008).
- [23] B. Dalena, J. Barranco, A. Latina, E. Marin, J. Pflingstner, D. Schulte, J. Snuverink, R. Tomás, and G. Zamudio, *Phys. Rev. ST Accel. Beams* **15**, 051006 (2012).
- [24] T. Shintake, *Nucl. Instrum. Methods Phys. Res., Sect. A* **311**, 453 (1992).
- [25] J. Yan, Y. Yamaguchi, Y. Kamiya, S. Komamiya, M. Oroku, T. Okugi, N. Terunuma, K. Kubo, T. Tauchi, and J. Urakawa, Conf. Proc. EAAC2013 (2013), (to be published) in *Nucl. Instrum. Methods Phys. Res., Sect. A*.
- [26] J. Snuverink, S. Boogert, Y. Kim, K. Kubo, A. Lyapin *et al.*, “Simulation and Measurement of Wake Fields at the Accelerator Test Facility 2” (to be published) in *Phys. Rev. ST Accel. Beams*.